

Study of Trajectory of Spin-Stabilised Artillery Projectiles

M. Krishnamurthy, D.G. Wakankar* and R. Sankar**

*Experimental Aerodynamics Division, National Aeronautical Laboratory
Bangalore-560 017*

ABSTRACT

Equations of motion for conventional spin-stabilised artillery projectile have been derived using a pseudo-stability axes system in addition to body-fixed and space-fixed axes systems. The aerodynamic forces and moments have been represented by their respective coefficients and the effects of Mach number and Reynolds number have been suitably accounted. The magnus terms which are significant at high rates of spin are estimated using a simple model. The set of equations have been partly linearised and solved numerically for a typical projectile using NAG system routines. Various trajectory parameters are computed and compared with the range-table data for the projectile. A parametric study has been carried out varying the aerodynamic coefficients to understand the sensitivity of the results obtained.

1. INTRODUCTION

In the history of warfare, the success or failure of a land battle can invariably be traced to the effective use or otherwise of artillery, and conventional spin-stabilised projectiles continue to be a major 'weapon' of the artillery world. On the battlefield of 1990s effective use of artillery would demand first round hit capability; quick switching of guns from one target to another; and extremely fast reaction to meet the

Received 6 December 1989, revised 23 March 1990

* Military Secretary's Branch, Army HQ, New Delhi-110 011

** Computer Science Department, University of Poona, Pune-411 007

requirements of highly mobile battles. These demands can be met by fast acquisition of the target, accurate computation of the gun data after accounting for all the known nonstandard conditions, and an equally efficient means of delivering the rounds on the target. The gun data computation using the tabulated data in the range-tables is a highly inefficient approach though commonly used by many countries. The process is manual, time consuming, involves interpolation errors and requires repetitive work for each firing. With the availability of sophisticated computers it should be possible to compute the complete gun data more accurately in a shorter time eliminating the possible human errors, thus achieving more effective neutralisation of the target.

The present work reports a general mathematical model developed to describe the motion of a spin-stabilised axisymmetric projectile and the resulting equations of motion which have been numerically solved to yield the complete trajectory of the projectile. The aerodynamic forces and moments are represented in terms of the corresponding coefficients and the effects of Reynolds and Mach numbers are suitably accounted. The Magnus terms which are significant at high rates of spin are incorporated based on a simple model. The method can give improved accuracy of predicting the point of fall and can be applied to any projectile of known aerodynamic characteristics.

2. EQUATIONS OF MOTION

Six-degree equations of motion for the projectile have been written making use of three systems of coordinate axes (Fig.1), viz space-fixed axes, body fixed axes, and an intermediate pseudo-stability axes. In the pseudo-stability axes system Y -axis always lies in the initial $X_0 Y_0$ plane and is not allowed to roll¹. The rigid-body linear and angular momentum equations for the projectile are written in the space-fixed coordinate system first, and are then transferred to body-fixed coordinate system, using the Eulerian angles—angle of yaw ψ , angle of pitch θ , and angle of roll ϕ —representing the orientation of the projectile in space. The effect of rotation of

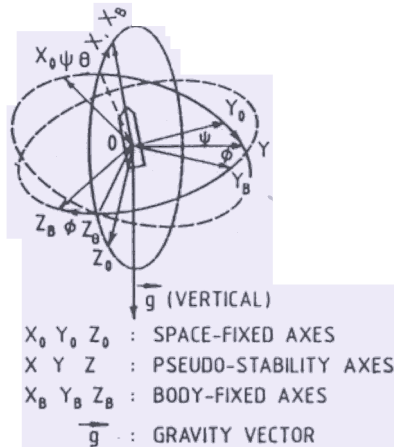


Figure 1. Axes system.

body-axes and pseudo-stability axes on the inertial terms are accounted for using Poisson's formula. The external forces include gravitational force and aerodynamic forces and moments. The details of the derivation are presented by Wakankar² (steps involved are outlined in the Appendix).

2.1 Aerodynamic Forces and Moments

The aerodynamic forces and moments are expressed in coefficient forms as

$$F_{AX,B,Y_B,Z_B} = \frac{1}{2} \rho V^2 S C_{X,Y,Z}$$

$$\mathcal{M}_{X_B,Y_B,Z_B} = \frac{1}{2} \rho V^2 S l C_{l,m,n} \tag{1}$$

where, the subscripts X, Y, Z represent components along and about X, Y and Z axes, and l, m and n are the rolling, pitching and yawing moment components. C is the force or moment coefficient, V the projectile speed, ρ the surrounding air density and S and l are the reference area and length of the projectile respectively. Any aerodynamic force or moment coefficient in Eqn (1) can be, in general, expressed as :

$$C_a = C_{a0} + C_{a\alpha} \alpha + C_{a\beta} \beta + C_{a\dot{\alpha}} \left(\frac{\dot{\alpha}l}{2V} \right) + C_{a\dot{\beta}} \left(\frac{\dot{\beta}l}{2V} \right) \left. \vphantom{C_a} \right\} \text{First order aerodynamic terms}$$

$$+ C_{a\dot{p}} \left(\frac{pl}{2V} \right) + C_{a\dot{q}} \left(\frac{ql}{2V} \right) + C_{a\dot{r}} \left(\frac{rl}{2V} \right)$$

$$+ C_{a\alpha\dot{p}} \alpha \left(\frac{pl}{2V} \right) + C_{a\beta\dot{p}} \beta \left(\frac{pl}{2V} \right) + C_{a\dot{\alpha}\dot{p}} \left(\frac{\dot{\alpha}l}{2V} \right) \left(\frac{pl}{2V} \right) + C_{a\dot{\beta}\dot{p}} \left(\frac{\dot{\beta}l}{2V} \right) \left(\frac{pl}{2V} \right) \left. \vphantom{C_a} \right\} \text{Magnus terms}$$

$$+ C_{a\dot{p}\dot{p}} \left(\frac{pl}{2V} \right)^2 + C_{a\dot{q}\dot{p}} \left(\frac{ql}{2V} \right) \left(\frac{pl}{2V} \right) + C_{a\dot{r}\dot{p}} \left(\frac{rl}{2V} \right) \left(\frac{pl}{2V} \right)$$

$$+ \text{higher order terms} \tag{2}$$

where, p, q and r are the roll, pitch and yaw rates of the projectile (expressible in terms of ψ, θ and φ and their time derivatives); α and β are the angles of attack and side slip. The second and third subscripts represent derivatives with respect to the corresponding nondimensional variable, and (*) represents time derivative. The second order terms retained in Eqn (2) are the Magnus terms and are significant for large spin rates. The coefficients C_a are assumed to be independent of the motion variables and are only functions of flight Mach and Reynolds numbers. For bodies possessing 90° rotational symmetry, the following simplifications can be made for the coefficients :

$$C_{X\alpha} = C_{X\beta} = C_{X\dot{\alpha}} = C_{X\dot{\beta}} = C_{X\dot{p}} = C_{X\dot{q}} = C_{X\dot{r}} = 0$$

$$C_{Y\alpha} = C_{Y\beta} = C_{Y\dot{\alpha}} = C_{Y\dot{\beta}} = C_{Y\dot{p}} = C_{Y\dot{q}} = C_{Y\dot{r}} = C_{Y\dot{q}} \tag{3}$$

$$C_{l0} = C_{l\alpha} = C_{l\beta} = C_{l\dot{\alpha}} = C_{l\dot{\beta}} = C_{lq} = C_{lr} = 0$$

$$C_{m0} = C_{m\alpha} = C_{m\beta} = C_{m\dot{\alpha}} = C_{m\dot{\beta}} = C_{mq} = C_{mr} = C_{n0} = C_{n\alpha} = C_{n\beta} = C_{n\dot{\alpha}} = C_{n\dot{\beta}} = C_{nq} = C_{nr} = 0$$

$$C_{Y\beta} = C_{Z\alpha}; C_{Y\dot{\beta}} = C_{Z\dot{\alpha}}; C_{Yr} = -C_{Zq}; C_{m\alpha} = -C_{n\beta}; C_{m\dot{\alpha}} = -C_{n\dot{\beta}}; C_{mq} = C_{nr}$$

$$C_{X\alpha\varphi} = C_{X\beta\varphi} = C_{X\dot{\alpha}\varphi} = C_{X\dot{\beta}\varphi} = C_{Xq\varphi} = C_{Xr\varphi} = 0$$

$$C_{Y\beta\varphi} = C_{Z\alpha\varphi} = C_{Y\dot{\beta}\varphi} = C_{Z\dot{\alpha}\varphi} = C_{Yp\varphi} = C_{Zp\varphi} = C_{Yr\varphi} = C_{Zq\varphi} = 0$$

$$C_l = 0$$

$$C_{m\alpha\varphi} = C_{n\beta\varphi} = C_{m\dot{\alpha}\varphi} = C_{n\dot{\beta}\varphi} = C_{mp\varphi} = C_{nr\varphi} = C_{mq\varphi} = C_{nr\varphi} = 0$$

$$C_{Y\alpha\varphi} = -C_{Z\beta\varphi}; C_{Y\dot{\alpha}\varphi} = -C_{Z\dot{\beta}\varphi}; C_{Yq\varphi} = C_{Zr\varphi}; C_{m\beta\varphi} = C_{n\alpha\varphi}; C_{m\dot{\beta}\varphi} = C_{n\dot{\alpha}\varphi}; C_{mr\varphi} = -C_{nq\varphi} \quad (3)$$

2.2 Linearisation and Nondimensional Equations

Variables α , β , ψ , q and r are initially zero and are assumed to be small during the trajectory so that the equations can be linearised in these variables by ignoring the higher order terms. Variables V , θ and p are not small and the nonlinear terms in V and θ are retained. However, variation in p over the initial spin rate p_0 can be assumed to be small and linearisation can be carried out in the variable $(p-p_0)$. Equations are nondimensionalised using

$$u = \frac{V}{V_0}; \quad t^+ = \frac{t}{\tau}; \quad \tau = \frac{l}{V_0}; \quad D = \frac{d}{dt^+} \quad (4)$$

where V_0 is the muzzle velocity and t is the real-time, and they are given below in the final form :

$$Du - u\alpha D\alpha - u\beta D\beta + u\alpha D\theta - [u\beta \cos \theta - K_1 C_{X_{pp}} E_0 \sin \theta] D\psi - K_1 C_{X_{pp}} E_0 D\phi = K_1 u^2 C_{X_0} - K_1 C_{X_{pp}} E_0^2 - K \sin(\gamma_0 + \theta) \quad (5)$$

$$\beta Du + \left[u - \frac{K_1}{2} u C_{Y_{\dot{\beta}}} \right] D\beta - \frac{K_1}{2} E_0 C_{Y_{i\varphi}} D\alpha - \frac{K_1}{2} E_0 C_{Y_{\varphi}} D\theta + \left[u \cos \theta \left(1 - \frac{K_1}{2} C_{Y_r} \right) \right] D\psi = K_1 u^2 C_{Y_{\beta}} \beta + K_1 u \alpha E_0 C_{Y_{\varphi}} + K \psi \sin \gamma_0 \quad (6)$$

$$\alpha Du + \left[\frac{K_1}{2} u C_{Z_{\dot{\alpha}}} \right] D\alpha - \frac{K_1}{2} E_0 C_{Z_{\dot{\beta}}} D\beta - \left[u \left(1 + \frac{K_1}{2} C_{Z_q} \right) \right] D\theta - \frac{K_1}{2} C_{Z_{rp}} E_0 \cos \theta D\psi = K_1 u^2 \alpha C_{Z_{\alpha}} + K_1 u \beta E_0 C_{Z_{\beta}} + K \cos(\gamma_0 + \theta) \quad (7)$$

where

$$u = \frac{V}{V_0}, \quad K_1 = \frac{\rho S l}{2m}, \quad K = \frac{gl}{V_0^2}, \quad E_0 = \frac{p_0 l}{2V_0}$$

$$D^2 \phi - \sin \theta D^2 \psi = K_2 u C_{1p} (D\phi - \sin \theta D\psi) \quad (8)$$

$$D^2 \theta + E_0 \cos \theta \left(\frac{2I_{X_B}}{I_{Y_B}} - K_3 C_{m_{rp}} \right) D\psi - K_3 u C_{m_{\dot{\alpha}}} D\alpha - K_3 u C_{m_{\dot{\beta}}} D\theta - K_3 E_0 C_{m_{\dot{\beta}}} D\beta = 2K_3 u^2 C_{m_{\alpha}} \alpha + 2K_3 u \beta E_0 C_{m_{\dot{\beta}}} \quad (9)$$

$$\cos \theta D^2 \psi - \left[E_0 \left(\frac{2I_{X_B}}{I_{Z_B}} + K_3 C_{n_{\alpha p}} \right) \right] D\theta - K_3 u C_{n_{\dot{\beta}}} D\beta - K_3 u \cos \theta C_{n_r} D\psi - K_3 E_0 C_{n_{\dot{\alpha}}} D\alpha = 2K_3 u^2 \beta C_{n_{\beta}} + 2K_3 u \alpha E_0 C_{n_{\dot{\alpha}}} \quad (10)$$

where

$$K_2 = \frac{\rho S l^3}{4I_{X_B}}; \quad K_3 = \frac{\rho S l^3}{4I_{Y_B}} = \frac{\rho S l^3}{4I_{Z_B}}$$

g is the acceleration due to gravity, m the mass of the projectile and I its moment of inertia.

The kinematic equations relating the velocity components along $X_0 Y_0 Z_0$ to the motion variables are given in the nondimensional form by

$$DX_0 = ul(\cos \theta + \alpha \sin \theta) \quad (11)$$

$$DY_0 = ul(\psi \cos \theta + \beta) \quad (12)$$

$$DZ_0 = ul(-\sin \theta + \alpha \cos \theta) \quad (13)$$

The initial conditions for Eqns (5) to (13) are,

$$\text{at } t^+ = 0; \quad u = 1; \quad \dot{\phi} = p_0$$

$$\alpha = \beta = \theta = \phi = \psi = \dot{\theta} = \dot{\psi} = 0; \quad \text{and} \quad X_0 = Y_0 = Z_0 = 0 \quad (14)$$

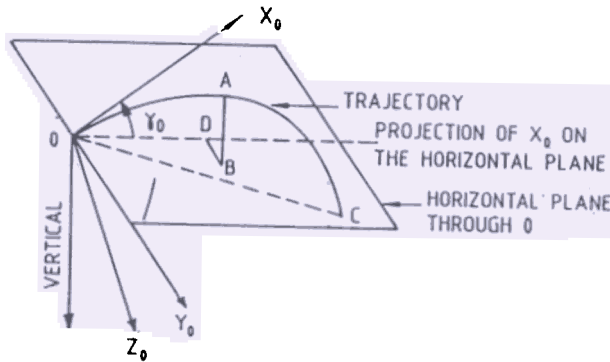
2.3 Solution

The set of Eqns (5) to (13) has been numerically solved on DEC-10 computer at IIT, Kanpur using Gear's variable-order-variable-step routine³ for a typical projectile for which aerodynamic data was partly available. All the first order aerodynamic coefficients except drag coefficient have been computed as per USAF Stability and Control Datcom method⁴ and the compressibility effects have been accounted using similarity rules⁵. The drag coefficient has been computed for different Mach numbers and Reynolds numbers⁶. The Magnus coefficients have been estimated

assuming a two-dimensional flow in the cross-flow plane². The temperature and density variations are chosen to correspond to ICAO atmosphere. The physical parameters of the trajectory shown in Fig. 2, viz range and height have been computed from the equations

$$\text{Range} = \sqrt{X_0^2 \cos^2 \gamma_0 + Y_0^2 + Z_0^2 \sin^2 \gamma_0 + X_0 Z_0 \sin 2\gamma_0} \quad (15)$$

$$\text{Height} = X_0 \sin \gamma_0 - Z_0 \cos \gamma_0 \quad (16)$$



- | | |
|------------|---------------------|
| O | POINT OF PROJECTION |
| C | POINT OF GRAZE |
| OC | RANGE |
| AB | VERTICAL HEIGHT |
| BD | LATERAL DEVIATION |
| γ_0 | ANGLE OF PROJECTION |

Figure 2 Geometry of the trajectory.*

A parametric study has been carried out by varying the aerodynamic coefficients one at a time to study the sensitivity of the results to these coefficients.

3. RESULTS AND DISCUSSION

3.1 Trajectories

Results have been computed for a muzzle velocity of 297 m/s and for angles of projection of 15, 25 and 30°, and are presented in Figs. 3 to 6. The initial spin rate is related to the muzzle velocity for a given gun and is accordingly set. The program takes on an average a CPU time of 3 to 4 s to execute a complete trajectory and write all the parameters at 1000 intermediate stations. In Fig. 3, the computed trajectories for the measured as well as theoretically estimated drag coefficients are presented and are compared with range-table data for three values of γ_0 . The computed trajectories for the two drag coefficients are quite close to each other, but they deviate

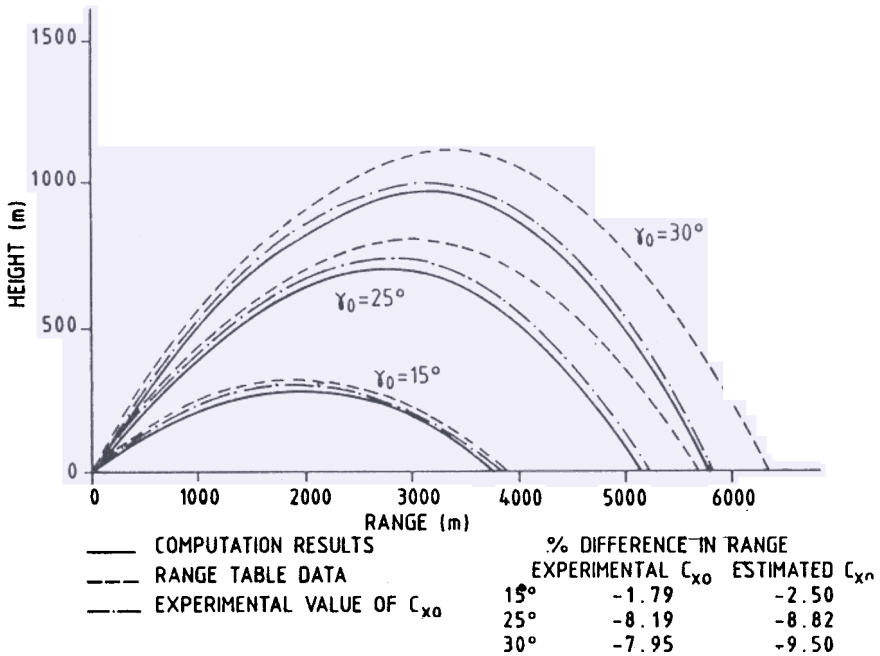


Figure 3. Height vs range; muzzle velocity = 297 m/s, $p_0 = 935.39$ rad/s.

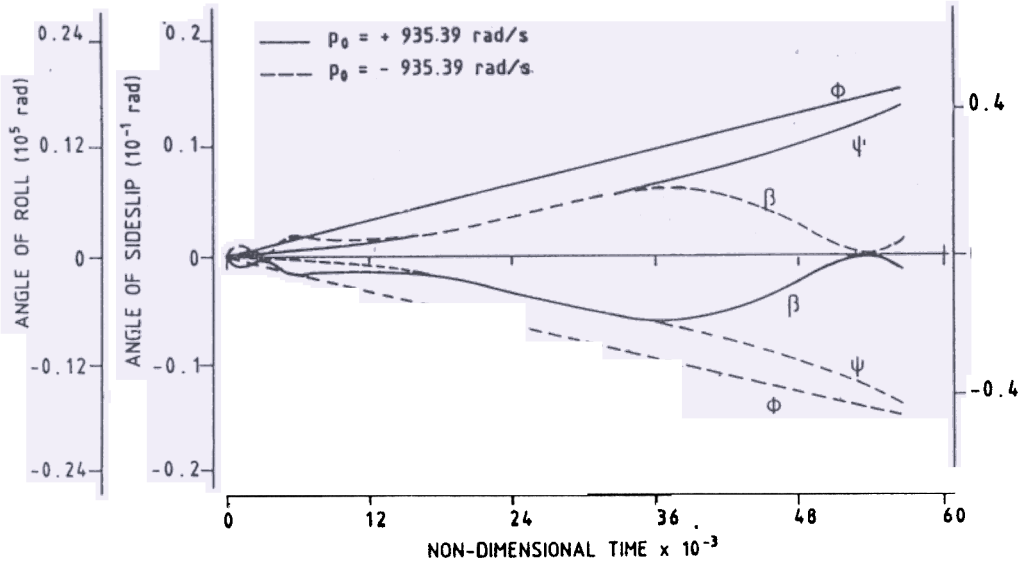


Figure 4. Time histories of lateral parameters, muzzle velocity = 297 m/s, $\gamma_0 = 25^\circ$.

considerably from the range-table plots for $\gamma_0 = 25$ and 30° . This difference builds up significantly during the second half of the trajectory and increases with increase of γ_0 initially. The computed results predict lower values of range and height than those of range-table results. Percentage deviation in range between the computed and range-table results are also presented in Fig. 3.

Figure 4 shows the time histories of the lateral parameters β , ψ and ϕ for a complete trajectory. It is observed that angle of yaw and roll angle build up continuously over the trajectory while the sideslip angle undergoes fluctuations. Similarly, it was observed in the case of longitudinal variables², that while pitch angle builds up continuously (negatively) with time, the angle of attack exhibits fluctuating variations. It was further noticed that θ variation with time is almost linear so that $\dot{\theta}$ can be approximated to zero for simplifying the model. Variation of ϕ with time in Fig. 4 is also seen to be almost linear implying that variation in spin rate is negligible. It is observed that the sideslip angle β remains small throughout the trajectory, so also the longitudinal parameter² a . These results justify the *a priori* assumption of small a , β , q and $(p - p_0)$. However, assumption of small ψ and hence small r seems to be in doubt from the observed results.

3.2 Effect of Magnus Terms

The influence of Magnus terms on the trajectory are shown in Figs. 5 and 6. In Fig. 5, variations of angle of attack and sideslip angle with time are presented with and without Magnus terms taken into consideration. In the absence of Magnus effect both a and β show variation with large fluctuations. While the angle of attack seems to settle down to a small steady state value in the later part of the trajectory, the sideslip angle still retains a large value at the end of the trajectory. The angle of attack variation with Magnus terms included is less fluctuating as compared to the variation without Magnus terms. This smoothening of the variation due to Magnus terms is even more pronounced in the case of sideslip angle variation. In Fig. 6, the significant influence of the Magnus terms on the lateral deviation Y_0 , has been presented. It is

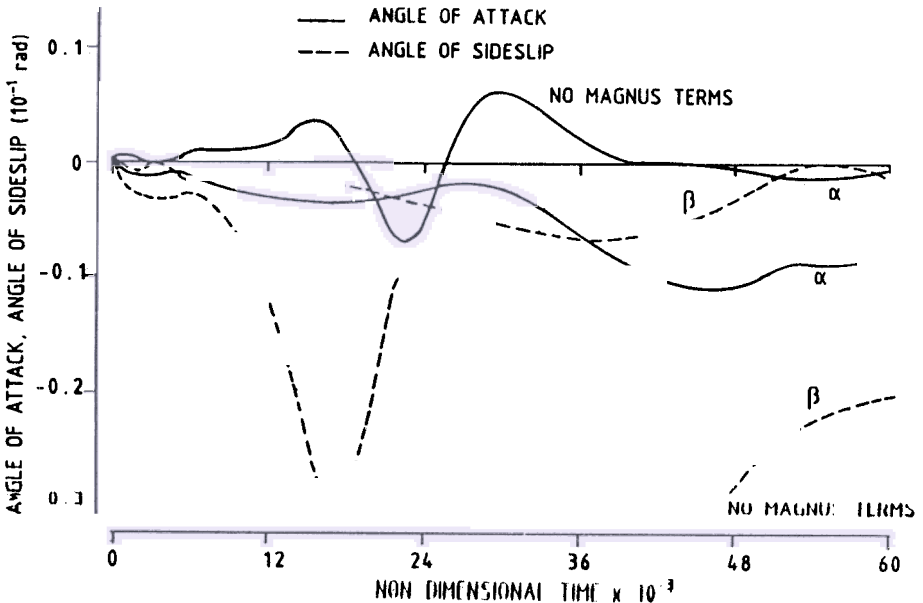


Figure 5. Effect of Magnus terms, muzzle velocity = 297 m/s, $p_0 = 935.39$ rad/s, $\gamma_0 = 25^\circ$.

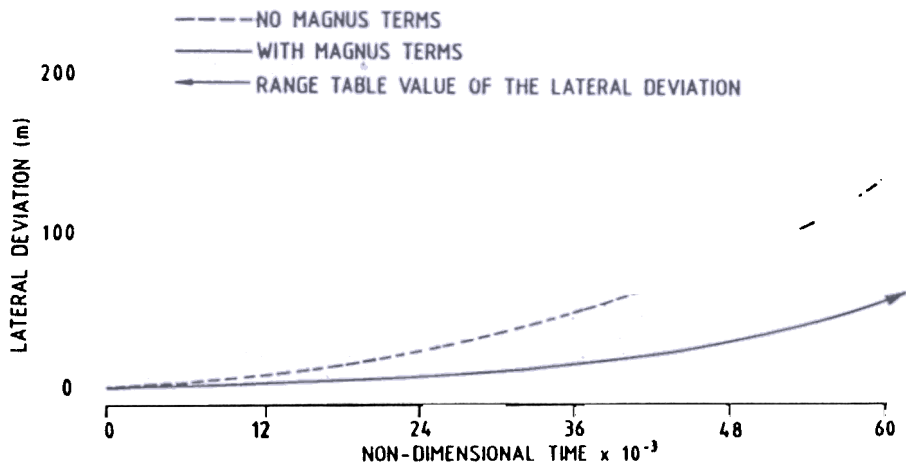


Figure 6. Effect of Magnus terms on lateral deviation ; muzzle velocity = 297 m/s, $p_0 = 935.39$ rad/s, $\gamma_0 = 25^\circ$.

noticed that while the lateral deviation builds up gradually along the trajectory for both the cases, the Magnus effect brings down the magnitude of the lateral deviation considerably, and the value of Y_0 with the Magnus effect included is very close to the range-table data for the particular case studied here. This emphasises the need to include the Magnus effect terms in the analysis.

3.3 Parametric Study

Figure 7 shows the dependence of range and height on the drag coefficient C_{x0} . It is seen that a reduction in drag coefficient results in increase of range and height and vice versa. At lower drag coefficient, the changes are more than those at higher

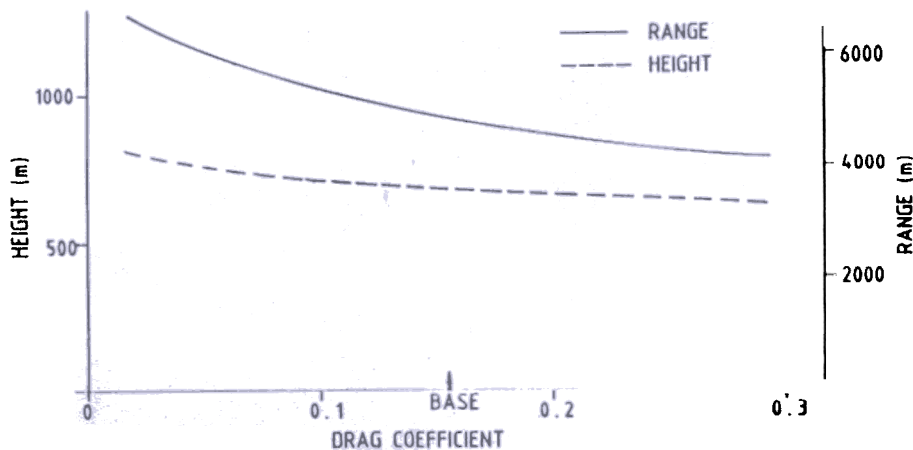


Figure 7. Effect of variation of the drag coefficient; muzzle velocity = 297 m/s, $p_0 = 935.39$ rad/s, $\gamma_0 = 25^\circ$.

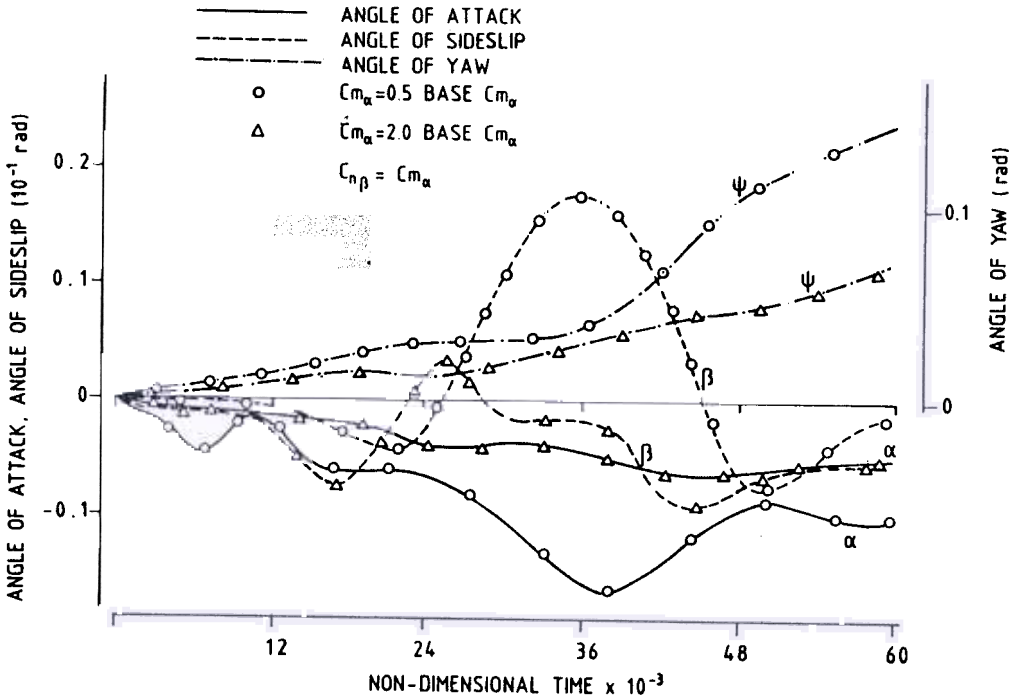


Figure 8. Effect of C_{m_α} ; muzzle velocity = 297 m/s, $p_0 = 935.39$ rad/s, $\gamma_0 = 25^\circ$.

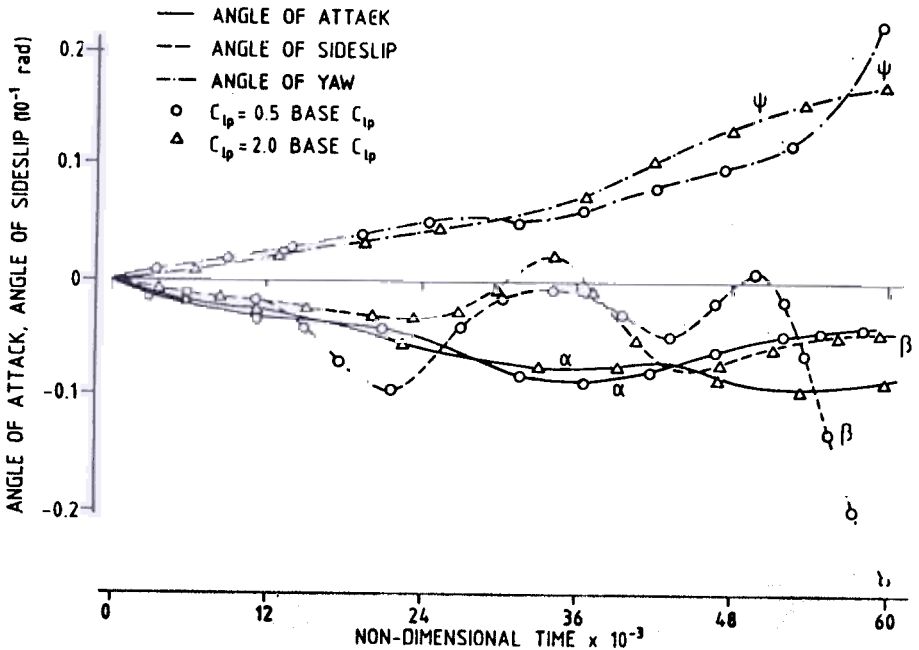


Figure 9. Effect of C_{l_p} ; muzzle velocity = 297 m/s, $p_0 = 935.39$ rad/s, $\gamma_0 = 25^\circ$.

drag coefficients. The drag coefficient is the most significant parameter in determining the trajectory; in particular the range mainly depends on it. Variation of C_{za} showed only small changes in the trajectory parameters: an increase of 90 per cent resulted in a 0.7 per cent reduction in range and 0.1 per cent reduction in vertex height. Similarly, variation of the parameters C_{za} , C_{ma} , $C_{m\dot{a}}$, C_{lp} , and C_{mq} independently did not show any significant changes in the overall trajectory parameters. However, variation in these parameters, except C_{mq} (and hence C_{nr}), did show significant changes in the variation of angle of attack, sideslip and yaw angle over the trajectory. Typical variations due to changes in C_{ma} ($= -C_{n\beta}$) and C_{lp} are depicted in Figs. 8 and 9 respectively. In these figures variations of α , β and ψ are plotted for half and twice the base values of C_{ma} and C_{lp} . Figure 8 shows that increase in C_{ma} ($-C_{n\beta}$) results in reducing the magnitudes of fluctuations in α and β considerably, owing to an increased level of static stability in pitch and yaw. Further, for large C_{ma} , the angle of attack and sideslip angle seem to settle down to steady state values towards the end of the trajectory, unlike, for small C_{ma} case. Increase of C_{ma} also results in a reduction of yaw angle ψ over the entire trajectory. From Fig. 9 it is seen that the roll damping C_{lp} mainly influences the sideslip angle variation. For lower roll damping the sideslip and yaw angles tend to diverge towards the end of the trajectory.

4. CONCLUSIONS

The discrepancy between the computed and range-table results can be mainly attributed to uncertainty in the data arising from variations in gun performance during repeat firing, limitations of measuring instruments, human errors, etc on one hand, and uncertainty in the aerodynamic data used in the computation on the other. Regarding the latter, methods used for estimation of Magnus terms and application of similarity rules to account for compressibility effects might be the contributing factors. It is observed from the results that, the perturbation quantities—angle of attack α , sideslip angle β , angular velocities $\dot{\theta}$ and $\dot{\psi}$ and also the change in the spin rate p' —are quite small and this justifies the postulates made in linearising the equations. However, assumption of small ψ and r seems to be in doubt from the observed results and needs a careful consideration. The observation that variation of θ with time is almost linear over the entire trajectory suggests that further simplification of the equations will be possible by neglecting $\dot{\theta}$ terms and assuming $\dot{\theta}$ to be constant. This study has brought out clearly the important role played by the Magnus terms and the need to include them in the analysis.

The parametric study has suggested that amongst the aerodynamic coefficients, the drag coefficient is the most critical parameter in determining the range and height of the trajectory and a precise determination of its value is essential for accurate prediction of the trajectory. Of the other coefficients, C_{ma} ($-C_{n\beta}$) and C_{lp} are found to influence the variations of α , β and ψ significantly over the trajectory. With a proper choice of coefficients, the present method can give very accurate results within 2% and the expensive and laborious exercise of preparing range-table can be obviated.

Further, the method can be used effectively on an on-field microprocessor thereby improving the success of firing a great deal. A rugged model of such a microprocessor will have no serious problems of power supply or stringent requirements of temperature and humidity for its operation and therefore, it will be feasible to use this on the battle-field very effectively.

REFERENCES

1. Charters, A.C. The linearised equations of motion underlying the dynamic stability of aircraft, spinning projectiles and symmetric missiles. NASA, Washington, D.C., 1955. 34 p. NASA-TN 3350.
2. Wakankar, D.G. Trajectory computation of spin-stabilised artillery projectiles. IIT, Kanpur, 1984. MTech Thesis. pp 10-28.
3. Numerical algorithms group. Fortran library manual, Mark 8, Vol. I, 1978.
4. US Air Force Stability and control DATCOM. Wright Patterson Air Force Base, Ohio, 1968.
5. Liepmann, H.W. & Roshko, A. Elements of gas dynamics. John Wiley and Sons Inc., New York, 1966. pp. 252-69.
6. Krasnov, N.E. Aerodynamics of bodies of revolution. American Elsevier Publishing Co. Inc., New York, 1970. pp. 379-401.

APPENDIX

EQUATIONS OF MOTION

In a moving axes system the equations of motion for a six-degrees-of-freedom motion vehicle can be written using the Poisson's equation as

$$\begin{aligned} \underline{\dot{M}} + \underline{\omega} \times \underline{M} &= \underline{F}_A + \underline{F}_G \\ \text{and } \underline{\dot{H}} + \underline{\omega} \times \underline{H} &= \underline{A}_A + \underline{A}_G \end{aligned} \quad (1)$$

where \underline{M} and \underline{H} are linear and angular momentum vectors respectively, and $\underline{\omega}$ the vector representing the angular velocity of the moving axes with components p , q and r . \underline{F} and \underline{A} represent the forces and moments respectively. Subscripts A and G stand for aerodynamic and gravitational contributions respectively. Equation (1) in section 2.1 describes these aerodynamic forces and moments. The gravitational moment \underline{A}_G will be zero if the centre of gravity of the body is chosen as the origin of the axes system. In what follows the steps involved in the derivation of the X -component force equation will be outlined.

X-Force Equation

X-component of Eqn (1) can be written as

$$\frac{dM_X}{dt} + q M_Z - r M_Y = F_{AX} + F_{GX} \quad (2)$$

The components of the linear momentum in Eqn (2) are given by

$$\begin{aligned} M_X &= mV_{XB} = mV[1 - \sin^2 \alpha - \sin^2 \beta]^{1/2} \\ M_Y &= mV_{YB} = mV \sin \beta \\ M_Z &= mV_{ZB} = mV \sin \alpha \end{aligned} \quad (3)$$

where m is the mass of the projectile and V the flight speed.

Following the assumptions of small α and β made in section 2.2, Eqn (3) can be approximated as

$$\begin{aligned} M_X &= mV \left(1 - \frac{\alpha^2 + \beta^2}{2} \right) \\ M_Y &= mV\beta \\ M_Z &= mV\alpha \end{aligned} \quad (4)$$

The angular velocity components in the body axes system can be expressed in terms of the Euler angles and their time derivatives using the familiar relationships as

$$\begin{aligned} p &= \dot{\phi} - \dot{\psi} \sin \theta \\ q &= \dot{\theta} \cos \phi + \dot{\psi} \sin \phi \cos \theta \\ r &= \dot{\psi} \cos \theta \cos \phi - \dot{\theta} \sin \phi \end{aligned} \quad (5)$$

For the pseudo-stability axes-system $\phi = 0$ (not allowed to roll) and hence Eqn (5) simplifies to

$$\begin{aligned} p &= \dot{\phi} - \dot{\psi} \sin \theta \\ q &= \dot{\theta} \\ r &= \dot{\psi} \cos \theta \end{aligned} \quad (6)$$

Substituting Eqn (4) and (6) in Eqn (2) and neglecting α^2 and β^2 terms we get

$$m \frac{dV}{dt} - mV \left(\alpha \frac{d\alpha}{dt} + \beta \frac{d\beta}{dt} \right) + mV \alpha \frac{d\theta}{dt} - mV \beta \cos \theta \frac{d\psi}{dt}$$

$$= \frac{1}{2} \rho V^2 S C_{ax} - mg \sin (\gamma_0 + \theta) \quad (7)$$

where C_{ax} is the X-component of the aerodynamic force coefficient. Making use of the results of Eqn (3) arising from 90° rotational symmetry, Eqn (2) in section 2.2 can be written as

$$C_{ax} = C_{X_0} + C_{X_{pp}} \left(\frac{pl}{2V} \right)^2 \quad (8)$$

Assuming the spin rate p to be different from the initial spin rate p_0 only by a small amount, one can write

$$p^2 \approx -p_0^2 + 2pp_0 \quad (9)$$

Substituting for p in the RHS of Eqn (9) from Eqn (6) we get

$$p^2 = -p_0^2 + 2p_0 \left(\frac{d\phi}{dt} - \sin \theta \frac{d\psi}{dt} \right) \quad (10)$$

Using the results from Eqn (8) and (10), Eqn (7) can be written as

$$m \frac{dV}{dt} - mV \alpha \frac{d\alpha}{dt} - mV \beta \frac{d\beta}{dt} + mV \alpha \frac{d\theta}{dt} - mV \beta \cos \theta \frac{d\psi}{dt}$$

$$\frac{1}{2} \rho V^2 S \left[\left(\frac{l}{2V} \right)^2 C_{X_{pp}} \left\{ 2p_0 \frac{d\phi}{dt} - 2p_0 \sin \theta \frac{d\psi}{dt} - p_0^2 \right\} \right]$$

$$- mg \sin (\gamma_0 + \theta) \quad (11)$$

Nondimensionalising Eqn (11) using the scheme defined by Eqn (4) results in

$$Du - u\alpha D\alpha - u\beta D\beta + u\alpha D\theta - [u\beta \cos \theta - K_1 C_{X_{pp}} E_0 \sin \theta] D\psi$$

$$- K_1 C_{X_{pp}} E_0 D\phi = K_1 u^2 C_{X_0} - K_1 C_{X_{pp}} E_0^2 - K \sin (\gamma_0 + \theta) \quad (12)$$

which is Eqn (5) of Section 2.2.

Derivations of Eqns (6)–(10) can be carried out in exactly similar manner as the one presented for Eqn (5), and have not been included here.